Molecular Simulation, Vol. 32, Nos. 3–4, 15 March–April 2006, 251–268

Taylor & Francis
Taylor & Francis Group

Multi-paradigm multi-scale simulations for fuel cell catalysts and membranes

W. GODDARD III*, B. MERINOV, A. VAN DUIN, T. JACOB, M. BLANCO, V. MOLINERO, S.S. JANG and Y.H. JANG

Division of Chemistry and Chemical Engineering, Beckman Institute (139-74), California Institute of Technology, Materials and Process Simulation Center, Pasadena, CA 91125, USA

(Received December 2005; in final form January 2006)

Dramatically improving the performance of fuel cell systems with their complex heterogeneous structures involving electrocatalysts, proton conducting membrane, reactant, and interfaces between them requires understanding the fundamental chemical, electrochemical, and physical phenomena at the heart of these complex materials and relating these fundamentals to the properties and performance of the membrane–electrode assembly. Our goal is to develop a predictive model that can be used to estimate the changes in performance upon changes in the design and which can be used to monitor performance of working fuel cells. Our strategy is to start with first principles quantum mechanics (QM) and to develop overlapping simulation methodologies in which QM is used to train a reactive force field that can be applied for large-scale (millions of atom) molecular dynamics simulations while retaining the accuracy of QM. The results of molecular dynamics are used to extract a coarse grain or mesoscale description useful in modeling properties at much larger scales. This model would enable the conception, synthesis, fabrication, characterization, and development of advanced materials and structures for fuel cells and for the associated hydrocarbon fuel reformers in an overall fuel cell system. We illustrate here some of the progress toward this goal.

Keywords: Polymer electrolyte membrane fuel cells; Computational modeling

1. Introduction

Polymer electrolyte membrane fuel cell (PEM-FC) systems have great promise for providing efficient environmentally acceptable portable power sources for transportation and related applications. However, despite quite significant investments in research and development, current systems lead to performance inadequate for the most important applications and the rate of progress is too slow. We propose an alternative paradigm for attacking this problem in which theory and simulation are used to predict from first principles the structural, transport, and electronic properties of full PEM-FC systems, allowing the materials and configurations to be optimized computationally prior to experimental synthesis and characterization. This will lead to current versus applied voltage characteristics for various materials choices, the proper measure of overall performance.

Our goal is to determine the fundamental processes of PEM fuel cells including:

- the catalytic reactions at the anode,
- the migration of the protons across the anode–electrolyte membrane interface,
- the transport properties of these protons (and fuel) as they traverse the electrolyte membrane,
- the migration of the protons onto the reactants and intermediates at the cathode, and
- the cathode based catalytic reactions to produce water.

Such studies of new materials and configurations require that the theory and simulation be based on first principles (since empirical data would not be available), which means that the fundamental description of the system must be based on quantum mechanics (QM). Until recently it would have been completely impractical to consider QM-based studies of the operation of fuel cells. However, a recent breakthrough in our laboratory provides the promise of making such simulations practical and accurate.

Recently, we have developed and validated the ReaxFF reactive force field to describe complex reactions (including catalysis) [1,2] nearly as accurately as QM but at costs comparable to force field (FF) based molecular dynamics (MD). This allows us to consider the fundamental processes for realistic descriptions of PEM fuel cells.

*Corresponding author. Fax: 1 626 586 0918. Email: wag@wag.caltech.edu

Molecular Simulation
ISSN 0892-7022 print/ISSN 1029-0435 online © 2006 Taylor & Francis
http://www.tandf.co.uk/journals
DOI: 10.1080/08927020600599709

Report Documentation Page

Form Approved
OMB No. 0704-0188

1. REPORT DATE	2. REPORT TYPE	3. DATES COVERED
JAN 2006		**00-00-2006 to 00-00-2006**

4. TITLE AND SUBTITLE	5a. CONTRACT NUMBER
Multi-paradigm multi-scale simulations for fuel cell catalysts and membranes	5b. GRANT NUMBER
	5c. PROGRAM ELEMENT NUMBER
6. AUTHOR(S)	5d. PROJECT NUMBER
	5e. TASK NUMBER
	5f. WORK UNIT NUMBER
7. PERFORMING ORGANIZATION NAME(S) AND ADDRESS(ES) **California Institute of Technology,Beckman Institute,Materials Process and Simulations Center,Pasadena,CA,91125**	8. PERFORMING ORGANIZATION REPORT NUMBER
9. SPONSORING/MONITORING AGENCY NAME(S) AND ADDRESS(ES)	10. SPONSOR/MONITOR'S ACRONYM(S)
	11. SPONSOR/MONITOR'S REPORT NUMBER(S)

12. DISTRIBUTION/AVAILABILITY STATEMENT
Approved for public release; distribution unlimited

13. SUPPLEMENTARY NOTES
The original document contains color images.

14. ABSTRACT

15. SUBJECT TERMS

16. SECURITY CLASSIFICATION OF:			17. LIMITATION OF ABSTRACT	18. NUMBER OF PAGES	19a. NAME OF RESPONSIBLE PERSON
a. REPORT	b. ABSTRACT	c. THIS PAGE			
unclassified	**unclassified**	**unclassified**		**18**	

These ReaxFF studies can be carried out for non-equilibrium systems in which current and protons flow so that one can address the current–voltage figure of merit relevant to FC performance. Each of these processes may require simulation models on the scale of 100 Å, requiring 100,000–1,000,000 atoms, but this is now feasible with ReaxFF. Such ReaxFF based studies of the dynamics would enable us to determine the fundamental processes at realistic electrode–electrolyte interfaces. Currently there is essentially no information about these interfacial processes, which we believe to be critical in determining fuel cell performance.

We have already validated that our theory and simulations reproduce some of the known properties of PEM-FC systems by simulating well-studied systems (e.g. Nafion membrane and Pt catalysts for anode and cathode) [3–5]. Now we are ready to use the theory and simulation to predict the properties of new systems in which catalysts are designed to provide lower barriers (overpotentials) with reduced effects of poisoning and in which the membranes are modified to optimize proton transport at higher temperatures while minimizing transport of fuel, oxidant and products.

This approach enables a new strategy for fuel cell development in which we consider the possibility of combinatorial computational design to test many possible alloys and membrane compositions computationally to find the best predicted performance as indicated by the overall current–voltage characteristics, followed by experimental synthesis and characterization on these best systems. Elements of our approach include:

- Overlapping simulation paradigms (figure 1), in which QM data are used to train first-principles based reactive force fields (ReaxFF) that are employed in large scale MD simulations to follow the reactive and transport processes at the heart of PEM-FC systems.
- Developing first-principles (*ab initio*) QM for proton transfer studies on model systems.
- Applying newly developed density functionals QM (X3LYP) for estimating the thermodynamics and kinetic energy barriers of proton exchange.
- Determining the fundamental chemical reaction mechanisms at the anode. This involves understanding each step from activation of the fuel to forming various intermediates and products. We will determine how this depends on surface defects and alloying. In addition, we will determine how each step is affected by solvent, electric field, and various potential poisons. Particularly important here are possible poisoning by heteroatom components in the fuel (S and N) and by reaction intermediates (CO). This understanding should allow us to suggest improvements in the anode catalysts.
- Determining the fundamental chemical reaction mechanisms at the cathode. The O_2 electroreduction at the cathode is kinetically slow ($\sim 10^2$ times slower than H_2 oxidation at the anode). Typically, the platinum catalysts consist of nanoparticles supported on a carbon electrode. We have already made some progress in determining the detailed mechanism of the cathode reactions on the Pt(111) surface and on multi-metallic (Pt/Ni, Pt/Co, Pt/Mo, etc.) alloys. We plan to extend these studies towards understanding the mechanism of the cathode reactions (including barriers) while including the effects of the carbon support and the presence of the electrolyte. We expect that such studies will lead to suggested improvements in the structure and composition of the cathode catalyst materials.
- Developing ReaxFF and hybrid classical/ReaxFF molecular dynamics (hybrid ReaxFF MD) to model the fundamental fuel cell chemistry while keeping the expense of the calculations relatively low.
- Developing MD and mesoscale methods for determining solubility, diffusion, and permeability of protons and water.
- Determining the kinetics for transport of protons, H_2O, fuel, fuel products, and O_2 through the PEM and how this depends on the nanostructure, concentration of water and salt, pH, temperature, and nature of the PEM.
- Characterization of how the nanostructure, heterogeneity, and properties of the PEM depend on polymer architecture.
- Detailed study of the interfaces between the electrode catalysts and the PEM with an emphasis on how this affects the transfer of the protons between the PEM and the appropriate reaction intermediates on the catalysts. This is likely the source of both overpotential and retarded voltage at high currents. We will then modify this interface by changing the catalyst and membrane to determine new materials that improve catalyst performance.
- Developing fuel cell models that allow us to suggest new leads for new electrolytic membranes to improve performance or to change the operating conditions (e.g. temperature). We consider new alternative membranes (such as the imidazole and dendrimer based modified electrolytes already suggested). Our goals are high-proton conductivity at appropriate temperature, low fuel and oxidant crossover, and excellent chemical and mechanical stability.
- Developing a full device fuel cell model based on the understanding of the fundamental processes (electrode

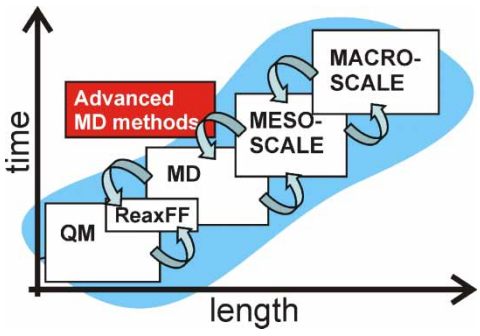

Figure 1. Overlapping simulation paradigms.

reaction kinetic, internal transport coefficients for protons, water, and fuel) to be obtained in the above studies. We focus on simulating the phase separation, morphology, interface structures of composites affecting the overall fuel cell performances.

For the most rapid progress, it is essential to couple these computational efforts to experimental tests of the predictions with the results of subsequent experiments fed back into the theory, perhaps leading to refined simulations aimed at resolving discrepancies or considering new phenomena. Ultimately this process of developing a complete computational model whose predictions have been validated by experiment will allow an accurate engineering model to be developed based on the theory and simulations but incorporating all the results obtained from experiments. Only with such wide-ranging collaborations between experiment and theory it will be possible to develop fully validated theoretical models for developing new materials and fully validated engineering models for optimizing performance.

2. Fundamental theory

In order to predict from theory, the properties of new materials (prior to synthesis) first-principles-based methods must be used. However, these models must be adequate to predict the large spatial and time scales relevant to devices. To accomplish this we use an overlapping hierarchy of computational methods involving different scales but each building upon the elements of a more fundamental description. Thus, the QM is used to determine the mechanisms of catalytic reactions and to predict the characteristics observable experimentally (e.g. XANES, EXAFS, NMR). In addition, the QM results are used to develop FFs for large-scale MD calculations. Similarly, MD results are used to extract properties for larger length and time scales (e.g. diffusion of H_2O and protons).

Additional developments are required in the QM study of the role of interfacial structures and applied voltages in electrocatalysis and the use of ReaxFF to describe the flow of protons between catalyst electrodes and electrolyte and within the electrolyte.

2.1 Density functional theory methods

We have used many QM methods to probe chemical reaction mechanisms and find that the B3LYP and X3LYP [6] flavors of DFT generally provide adequate accuracy at modest cost. We use this approach to characterize the catalytic processes at the anode and cathode. Our strategy here is to carry out QM calculations with the catalyst represented by clusters of $\sim$35 atoms [7] to determine the mechanism of the dispersed catalyst and then to do QM calculations on periodic slabs to describe (ordered) overlayers on infinite surfaces. For the finite clusters, we use Poisson–Boltzmann continuum solvent methods to provide an accurate description of solvent polarization. We have applied this successfully to reactions in water and sulfuric acid, where it leads to solvation energies (for neutral species) good to $\sim$0.5 kcal/mol and to pK_a values good to $\sim$0.5. We also use these methods to describe the elementary steps for proton transfer through the electrolyte.

For periodic calculations, we prefer the SeqQuest code being jointly developed at Sandia National Labs (Peter Schultz) [8] and at Caltech, and the Crystal2003 software [9]. Both allow the use of Gaussian basis functions and hard or soft pseudopotentials.

2.2 First principles-based reactive force field (ReaxFF)

The QM calculations described above are useful for characterizing idealized electrochemical processes (involving simple, ordered structures, zero temperature, etc.). However, these methods are too slow for routine studies of the fundamental unit processes that characterize FC performance under actual operating environments (i.e. realistic electrode–electrolyte interfaces, finite temperature, disordered structures, longer time-scales). MD calculations using FFs provide a computationally efficient way of describing the dynamics with large-scale simulations. However, FFs have not generally been capable of accurately describing chemical reactions. Recently, we have made a breakthrough in this area with the development of the ReaxFF capable of reproducing high-level QM data for reactive and non-reactive systems. ReaxFF descriptions have already been reported for a wide range of systems, including hydrocarbons [10], nitramines [11], peroxides [12], aluminum metal and aluminum oxides [13], silicon metal/silicon oxides [14] and silicon carbides [1], copper/nickel/cobalt interactions with carbon [2], magnesium and magnesium hydrides [15], lithium/-lithium carbides [16] and all-carbon materials [17] while ongoing developments are extending the methodology further across the periodic table (figure 2), including reactions on Pt, Pt_3Co, Pt_3Ni, PtRu, and $BiTeO_x$ surfaces. In addition a similar methodology provides an excellent description of a $BaTiO_3$ ferroelectric materials [18].

This progress demonstrates that a wide range of reactions and reactive systems can be described using essentially the same FF. ReaxFF has also been re-coded for a parallel environment, and fully reactive simulations of around half a billion atoms have been reported [19], suggesting that realistic simulations covering the full complexity of the fuel cell environment are now feasible.

The ReaxFF-description involves the following three types of interactions:

a. *Environment dependent charge distributions on atoms.* The charge on each atom is described with a Gaussian shape to provide for proper shielding as the atoms come close together. This allows the electrostatic interactions of bonded atoms to be included, eschewing the common approach of "excluding"

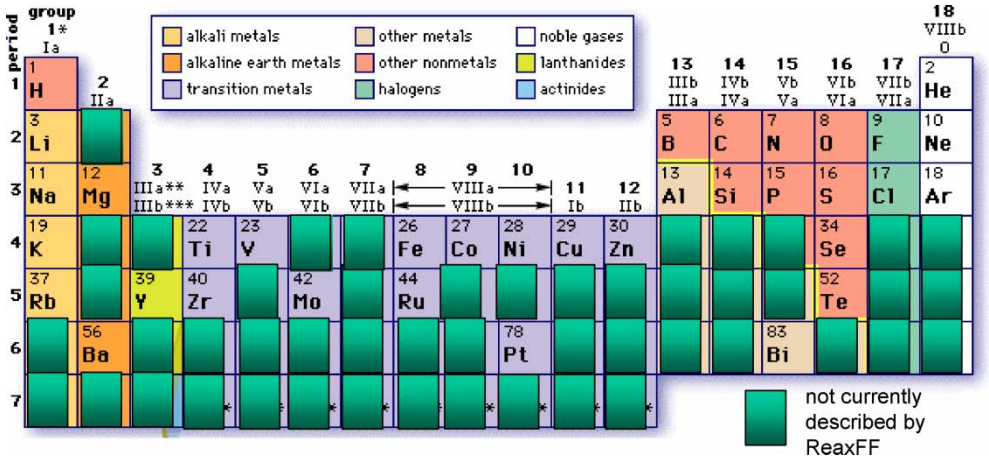

Figure 2. Atoms currently described by the ReaxFF method.

bonded atoms from the electrostatics. The charge of the atom is allowed to transfer to other atoms in response to the local environment of each atom [as in the charge equilibration (QEq) model]. Such proper description of electrostatics is essential in describing systems undergoing oxidation and reduction, as in fuel cells.

b. *Bond-order dependent valence terms.* All valence terms (bonds, angles, torsions) go to zero, as the bonds are broken, allowing a smooth description of chemical reactions. The bond orders are determined only by the interatomic distances and are updated every iteration, allowing ReaxFF to automatically recognize and handle changes in connectivity as reactions proceed.

c. *General non-bond van der Waals interactions.* To account for short range Pauli repulsion and longer range dispersion interactions we use a universal *v*d*W* term that applies to every atom pair, independent of bonding (again no exclusions). These terms are also shielded to properly describe the changes at short distances.

The following guiding principles were used in the ReaxFF development:

d. *Every parameter is derived solely from QM.* A critical aspect of the ReaxFF is that it is based solely on *ab initio* QM calculations and parameterized to reproduce a large number of reactions designed to characterize the atomic interactions under all possible environments an atom might encounter.

e. *Transferable potential.* Each element is described by just one atom type. That is there is one set of carbon FF parameters, which automatically describe correctly C in diamond and graphite, organics like ketones and allyl radicals, the carbide on top of a Ni surface. This is necessary since the reactions may interconvert between all of these forms.

f. *No predefined reactive sites.* Since the concept of bonds and reactions arises naturally in terms of the interactions (just as in QM) the user does not predefine where and when reactions are expected to occur. Thus ReaxFF allows unbiased simulations of reactive systems.

g. *No discontinuities in energy or forces.* Even during reactions, ReaxFF provides a continuous energy and force description, thus allowing proper reactive MD simulations.

Recently, we have developed ReaxFF potentials covering the following aspects of PEM-FC chemistry:

(1) *Reactions at metal surfaces.* To enable a large-scale dynamical description of the chemical events at fuel cell metal anode and cathode we have developed ReaxFF for Pt/C/H/O, Ru/H/O and Ni/C/H/O interactions.

(2) *Oxidation/reduction reactions.* To ensure that ReaxFF describes redox reactions accurately, we have fitted ReaxFF against a wide range of metal oxidation states.

(3) *Hydrogen transport.* The approach that we have used to predict proton transport through complex membranes such as Nafion is to use QM to determine the barriers for H migration as a function of the donor–acceptor separation and then to combine probabilities based on these results with MD studies, allowing proton transport to occur when appropriate configurations are encountered.

With ReaxFF we do not need to separate these processes, since the reactions can occur during the dynamics. To validate the application of ReaxFF to hydrogen transport through electrolytes figure 3 compares QM and ReaxFF results for H-migration between an imidazole and an imidazolium cation as a function of nitrogen–nitrogen distance [20]. This shows that ReaxFF properly describes the distance dependent hydrogen migration barriers, indicating that ReaxFF can be used to describe reactive transport through fuel cell electrolytes.

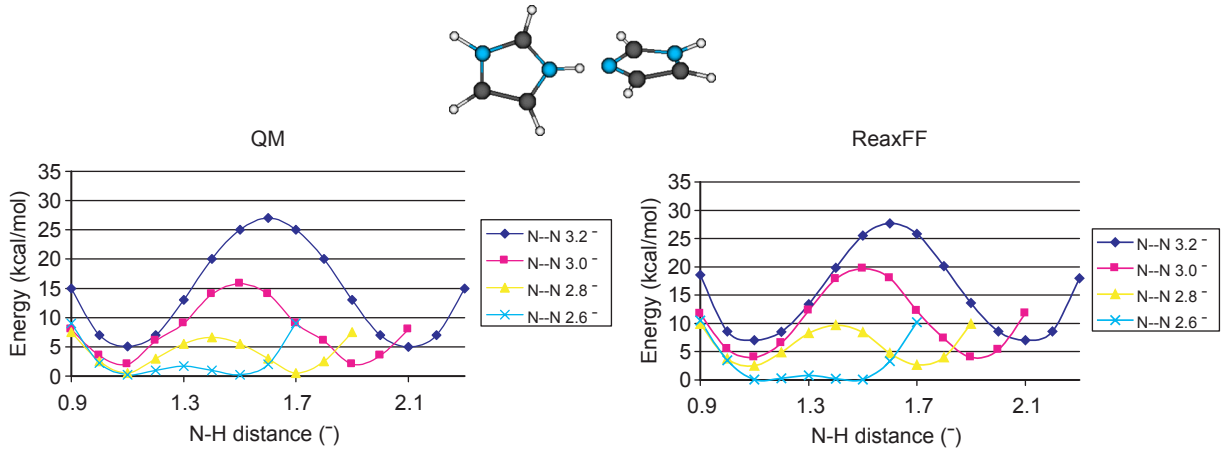

Figure 3. QM and ReaxFF energies for hydrogen migration barriers between an imidazolium cation/imidazole pair as a function of nitrogen–nitrogen distance.

Since the ReaxFF applies to all combinations of the elements, the ReaxFF descriptions of separate components of PEM-FCs can be used on the composite systems, allowing the ReaxFF based simulations for studying the critical chemical events at PEM-FC interfaces.

2.3 Large-scale molecular dynamics simulations

MD simulations using the accurate ReaxFF will provide a first-principles characterization of the fundamental processes (structures, mechanisms, energetics, and rates) and mechanisms in a FC including:

1. Polyelectrolyte membranes
   a. Microstructure of hydrated polymers (Nafion®) and new alternative membranes;
   b. Proton transport in hydrated polymer (Nafion®) and new alternative membranes:
      (1) Mechanisms;
      (2) Role of water/water transport.
2. Anode/electrolyte interfaces
   a. Obtain atomistic structures of the interface between the anode, electrolyte, gas (fuel);
   b. Characterize the chemistry at the three-phase interface under realistic operating conditions (this includes the migration of the proton to the electrolyte and the detailed reaction steps on the catalyst).
3. Cathode/electrolyte interfaces
   a. Obtain atomistic structures of the interface between the cathode, electrolyte, gas (O_2);
   b. Characterize the chemistry at the three-phase interface under realistic operating conditions (this includes the migration of the proton from the electrolyte and the detailed reaction steps on the catalyst).

Many of these applications require large-scale MD simulations on 10,000–1,000,000 atoms. These will be based on our recently developed computational materials design facility (CMDF) that allows a mixture of paradigms and scales to be utilized simultaneously to describe the time evolution of large scale complex reacting systems. This framework allows the facile mixture of complex independent software codes development for a various paradigms (QM, ReaxFF, classical FF, mesoscale FF, finite element analysis) to be used independently but simultaneously on the same problem.

3. Computational modeling of electrode/electrolyte interfaces

To develop the capability for modeling the electrode/electrolyte interface in a PEM-FC we examine the properties of Nafion hydrated polymer as membrane and Pt catalysts as the electrode material. There is a great deal of data on Nafion and Pt for both cathode and anode in a PEM-FC, but little microscopic understanding of the properties. This availability of experimental data allows us to check reliability of our first-principles based model by comparing to experiment.

3.1 Nanostructure and transport properties of Nafion

Although great progress has been made since the pioneering work by Gierke on the Nafion structure in 1980s [21], the details of the microstructure of hydrated Nafion remain highly disputed. The main function of the electrolyte membrane in a fuel cell is to provide high proton conductivity, electrochemical and mechanical stability, and a barrier for transport of electrons, fuel, and oxidant. Despite its high cost and restriction to work at temperature not higher than 80°C, Nafion remains the material of choice for fuel cell applications.

Nafion is a polyelectrolyte consisting of non-polar tetrafluoroethylene (PTFE) segments, $N = (CF_2{-}CF_2)$ and polar perfluorosulfonic vinyl ether (PSVE) segments, $P = (CF_2{-}CF(O{-}CF_2{-}CF(CF_3)){-}CF_2{-}CF_2{-}SO_3H)$ that are easily ionized in water. The properties of hydrated Nafion are due to its nanophase-segregated structure in which hydrophilic clusters are embedded in a hydrophobic

matrix. We have characterized the nanostructure, segregation, position of the ionic groups, and water distribution of the hydrated Nafion membrane using non-reactive FF MD simulations [4]. It was found that the monomeric sequence of the Nafion chain (i.e. the block segregation of hydrophobic and ionizible groups along the linear polymer chain) affects the nanophase-segregation structure and transport in this material. We carried out MD simulations of Nafion using two extreme monomeric sequences: the first one was very dispersed and the second was very blocky (figure 4).

The monomer sequence influences the water mobility by affecting the membrane nanosegregation. We computed the water diffusion coefficients and found that the dispersed (low blockiness) membrane is ~25% smaller than for the blocky case (0.46×10^{-5} vs. 0.59×10^{-5} cm^2/s at 300 K). The experimental value, 0.50×10^{-5} cm^2/s, is within the calculated range. On the other hand, the vehicular diffusion of hydronium is not affected significantly by the monomeric sequence.

We have also characterized the structure of the water in the Nafion membrane as a function of the water content and found that the hydrophobic domains percolate for water content above 3–5 water molecules per a sulfonate group. We consider that this percolation of the hydrophilic domain is essential to provide the pathways for proton diffusion responsible for the experimentally observed increase of the proton conductivity above ~3 water molecules per sulfonate group in Nafion.

Our atomic level characterization of the microstructure of hydrated Nafion and its effect on the diffusion of water and vehicular diffusion of protons provides the base for proposing to

a. Parameterize the ReaxFF to fit QM calculations on Pt, hydrated Nafion, and the interface between them with particular emphasis on an accurate description of the proton transfer processes. This is a key step toward integrating the reactivity and dynamics of the proton migration into the ReaxFF framework;
b. Characterize the pathways of proton diffusion inside the membrane. Of particular relevance is the mechanism of proton transfer through the narrow channels connecting the hydrophilic domains at intermediate water content. For high water (>7 H_2O per SO_3) the proton transport depends little on the SO_3 groups (except to provide the protons), however our simulations suggest that at low water, the sulfonate moieties may play an important role in allowing percolation of the proton networks;
c. Using ReaxFF compute the proton transfer rates as a function of the channel width and sulfonate distribution. This information is used to develop a mesoscale model for Nafion membrane;
d. Develop an electrode potential dependent parameterization of the ReaxFF to study the electrochemical reactions at different applied potentials;
e. Determine the mechanism of the proton transfer at the interface, and the electrochemical reactions at the electrodes; and
f. Determine water-replacement polyelectrolytes capable of high operational temperatures (>120°C) and high proton conductivities (>0.1 S/cm).

3.2 *Modeling of Pt and Pt-alloy electrodes*

Despite great effort to find alternative efficient catalysts for PEM-FC applications, Pt and Pt-based alloys remain the only catalysts capable of generating high rates of chemical reactions at relatively low operating temperatures (~80°C) of PEM-FCs. We have used QM to describe such catalysts in two complementary ways: (1) finite clusters containing ~35 metal atoms, and (2) infinite slabs having the thickness of 3–5 layers of metals, and using periodic boundaries.

The finite cluster calculations are more useful for establishing the detailed sequence of reaction steps because more accurate hybrid levels of DFT are available. In addition such clusters describe the highly dispersed Pt-nanoparticles (2–5 nm) being used.

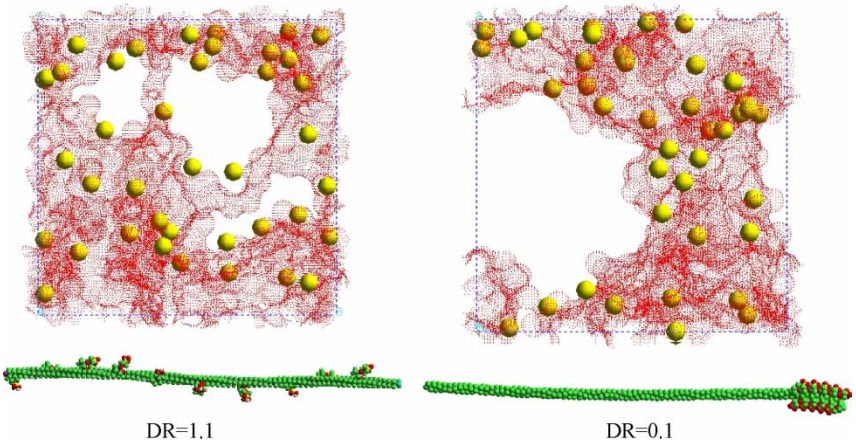

Figure 4. Nanostructure of hydrated Nafion. White domains are mainly occupied by the Nafion backbone. Spheres represent sulfur atoms. The surface formed by dense dots is the Nafion/water interface.

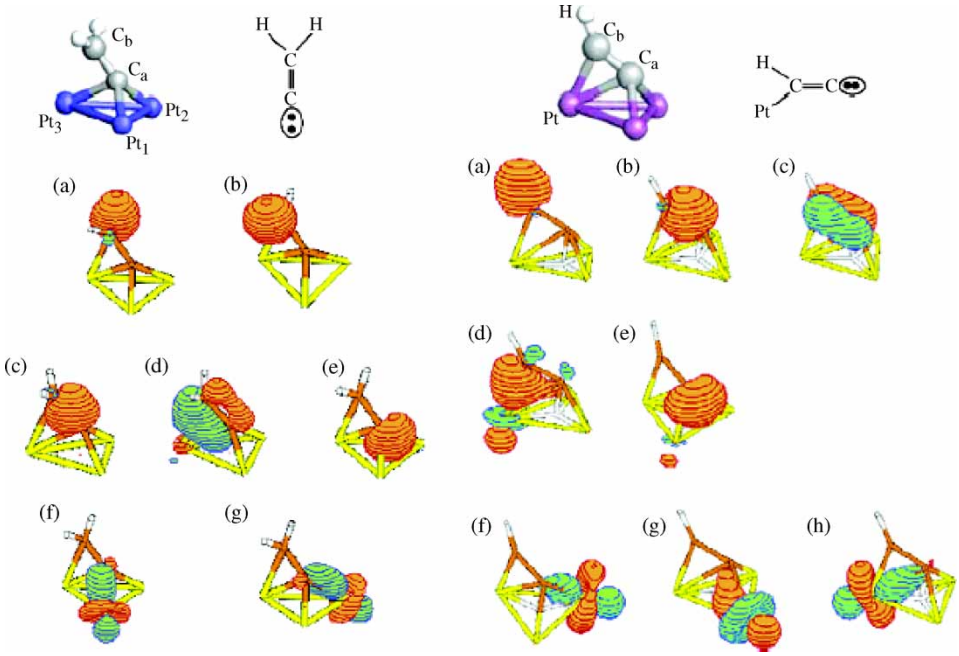

Figure 5. Analysis of the occupied orbitals for the $Pt_3{-}CCH_2$ and $Pt_3{-}CCH$ systems.

Periodic slabs are most useful when comparing to surface science experiments and for describing the processes at electrodes. Generally, we do some calculations using both approaches to allow crosschecking.

We have carried out a number of QM calculations describing a Pt-catalyst using a finite cluster, increasing systematically the number of cluster-atoms and examining both the electronic structure of the surface cluster and reactions, to find the smallest suitable cluster [7]. Our conclusions from these studies is that the minimum size for a cluster to accurately describe chemisorption is the three-layer system $Pt_{9.10.9}$ (28 atoms), which leads to adsorption energies, bond distances, and vibrational frequencies similar to the infinite Pt(111)-surface. To describe surface reactions of organic molecules on the catalyst surface [e.g. Pt(111)] requires a slightly larger cluster with 35 atoms, $Pt_{14.13.8}$-cluster, allowing calculation of reactions on the surface while minimizing side effects.

In addition, based on the interstitial electron model (IEM) of McAdon and Goddard [22] as extended by Kua and Goddard [23], we have developed an orbital model of the Pt surface that explains its reactivity for reforming various hydrocarbons [24]. Figure 5 shows examples of orbitals obtained from a Pipek–Mezey localization of the occupied orbitals for $Pt_3{-}CCH_2$ and $Pt_3{-}CCH$.

3.2.1 First principles study of fundamental reactions at Pt-anode catalyst. We have already carried out QM calculations on the surface reactivity of the Pt and PtRu anode catalysts. This QM uses a new *ab initio* DFT-GGA method (X3LYP) [6], which more accurately describes such weak and non-bonded interactions as van der Waals dispersion. In order to represent the surface of the catalyst finite clusters and periodic slabs will be used. The overall chemical reaction at the anode in a direct methane FC is:

$$CH_4 + 2H_2O \rightarrow CO_2 + 8H^+ + 8e^-.$$

We previously used QM on small clusters to examine the role of various intermediates. We now extend these results to the 35-atom clusters (figure 6). In addition to activating the CH bond of CH_4 and the OH bond of H_2O, what is particularly important is the final step of forming the CO_2 product. We need to avoid forming CO, which both poisons the surface and reduces efficiency. We are particularly interested in the possible role of oxidized and hydrated Ru clusters being formed under reaction conditions. These may play a role in directing the second O to form CO_2 and in transporting the proton from the catalyst to the electrolyte.

To determine the coverage dependencies and the influence of pre-adsorbed species, we use periodic slab-calculations.

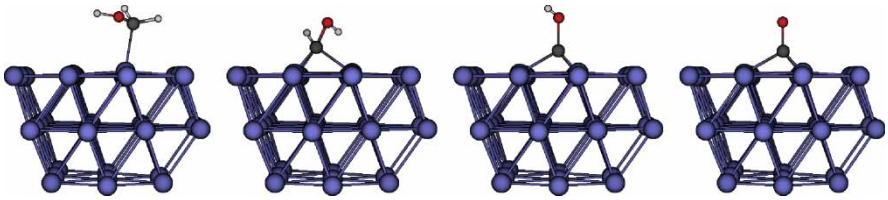

Figure 6. CH_2OH, CHOH, COH, and CO intermediates on Pt(111).

These calculations can also include solvation effect through the Poisson–Boltzmann methods.

Most important here is that the QM results are used to train the ReaxFF reactive force field. This allows us to simulate very complex systems with 10,000–1,000,000 atoms, far too large for QM, and to examine the migration of fuel to the electrode and reacting while also treating transport of the fuel through the membrane simultaneous with the protons and water.

In addition to the basic Pt and PtRu systems, we plan to explore how doping with other elements might change the processes to minimize poisons while lowering barriers to the reactions and the transport of protons and increasing barriers for transport of fuel. We expect that this will lead to new strategies that can be tested experimentally to develop improved anode catalysts.

3.2.2 Atomistic level modeling of cathode catalytic reactions. The major source of inefficiency in PEM-FC remains to be the significant overpotentials (excessive reaction barriers) in the PEM-FC cathode reaction of protons flowing through the membrane to convert dioxygen (O_2) to water.

$$O_2 + 4H^+ + 4e^- \rightarrow H_2O,$$

(both for H_2 and CH_3OH fuel). This four-electron reduction process involves a complex multi-step sequence in which there remains significant uncertainty regarding the reaction mechanism. Despite great efforts to find alternative catalysts to promote a high rate of oxygen reduction, Pt-based materials remain the best for the relatively low temperatures (~ 80°C) at which PEM-FCs operate. The performance of PEM-FCs is primarily limited by the slow rate of the O_2 reduction half reaction, which is 10^2 times slower than the H_2 oxidation half reaction. Therefore, it is very important to understand the reaction processes at the cathode in order to find a sequence that would maintain a small barrier for each step.

We used 35-atom clusters to determine the binding energies and structures for each possible intermediate (O, H, O_2, H_2, OH, OOH, H_2O) involved in the cathode reaction on the Pt(111) surface and some of these intermediates on the Pt_3Ni and Pt_3Co alloy catalysts. We find that atomic oxygen is most strongly bound at the μ_3-fcc position, while molecular O_2 prefers the bridge site. OOH prefers the same geometry as O_2 with one O covalently bound on top of a Pt atom (24 kcal/mol). Including zero-point energy (ZPE) a single H atom prefers the μ_3-fcc site over an on top site by 3.2 kcal/mol, whereas molecular H_2 undergoes dissociation to two on top bound H atoms wile adsorbing on Pt. OH and water show comparable binding structures (on top bound), but a different type of binding. The hydroxyl radical is covalently bound to one Pt atom (47 kcal/mol), and water uses the remaining lone pair orbital of its oxygen to attach to the surface atom (14 kcal/mol).

In order to determine the complete reaction pathway, we calculated all possible dissociation processes of the various intermediates on the Pt-cluster. Using this energetics we calculated heats of formation (ΔH_f) and combined them with the dissociation barriers. Since oxygen and hydrogen react catalytically at the cathode to form water, we determined possible reaction pathways starting with gas-phase H_2 and O_2. We distinguished two main gas-phase reaction pathways: (1) O_2-dissociation, figure 7(a) and (2) OOH-formation, figure 7(b).

Along the O_2-dissociation pathway dioxygen adsorbs on the surface, then dissociates, and finally reacts with chemisorbed hydrogen atoms to form water. The rate-determining step for this mechanism is the $O^{ad} + H^{ad} \rightarrow OH^{ad}$ reaction with a barrier of 32 kcal/mol rather than the dissociation of O_2, whose barrier is only 15 kcal/mol.

Along the OOH-formation pathway, a surface hydrogen first reacts with adsorbed O_2 to form OOH, which dissociates to form chemisorbed OH and O. These finally react with other chemisorbed hydrogen to from water. In this mechanism the $OOH^{ad} \rightarrow OH^{ad} + O^{ad}_{fcc}$ dissociation step has the highest barrier of 17 kcal/mol. Therefore, the OOH-formation mechanism seems favorable for the cathode reaction. The results discussed above were for the gas phase processes, which we use as the starting point for examining the cathode reaction mechanisms under conditions suitable for fuel cells. Fuel cells are dynamic systems in which the catalytic particles at the electrode can directly contact parts of the membrane and surrounding water medium. Thus we must include the effects of solvation and of external electric field (figure 8).

First, we use DFT in combination with the self-consistent reaction field (SCRF) from Poisson Boltzmann theory to describe the solvation effects for a hydrated environment and determine the structural and energetic changes due to solvation. For example, the structure of a layer of adsorbed water molecules on Pt surface changes drastically upon solvation and the binding energy to the surface decreases significantly. Polarized species, such as chemisorbed HO_2 intermediate show especially large changes in the structure, binding, and dissociation energies due to solvation.

The water environment also changes the charge distribution of the surface species, leading to both increases and decreases in the binding to the surface, which changes the corresponding reaction barriers. Some areas of the catalyst surface might be hydrophobic due to nearby fluorocarbon regions of the membrane; these regions may prefer O_2. Here, the reaction mechanism may resemble that in the gas-phase. Other regions may be hydrophilic due to nearby water channels and sulfate groups. Here solvation may drastically change the reaction pathways. Some reaction steps may occur in hydrophobic interface areas while the others may prefer hydrophilic areas. We must utilize both sets of energetics and dissociation barriers (gas-phase and solution) to describe fuel cell performance.

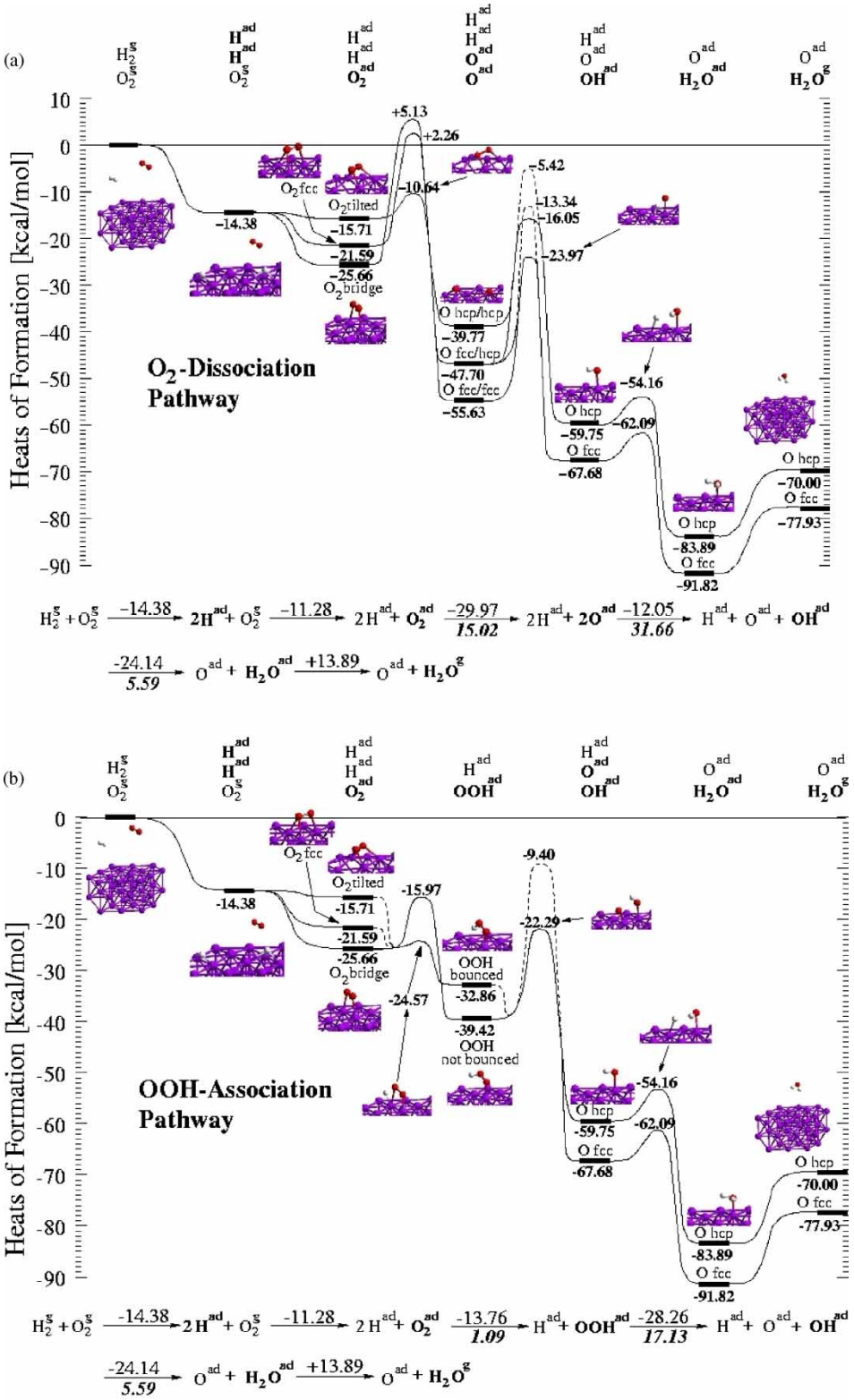

Figure 7. (a) Energetics for the O_2-dissociation pathway on the Pt_{35}-cluster. (b) Energetics for the OOH-dissociation pathway on the Pt_{35}-cluster.

To complete the picture of the cathode mechanism, we must model the effect of the electric field under fuel cell operating conditions. Thus for calculations in which the catalyst is treated as a slab, we add the electric field to the QM or FF Hamiltonian, which has the effect of modifying the effective chemical potential (Fermi energy) as a function of the distance from the metallic catalyst surface. For cases in which a cluster is used to describe the catalysts, we can treat the effect of the field on the reactions at the catalyst surface by changing the net charge on the catalyst (the gas phase calculations were carried for systems with zero net charge). Calculations of adsorbed water on Pt(111)

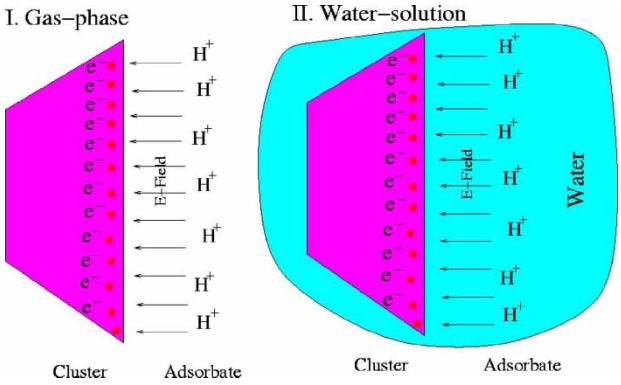

Figure 8. Method to model solvation and electric field.

clusters with various net charges show significant changes in the orientation of the water molecule (figure 9). We will carry out similar studies for all intermediates involved in the reaction at the conventional Pt-electrode. Since the reaction processes on the Pt-electrode have been well studied experimentally, we use Pt to validate our methodologies for the complete set of cathode reaction mechanism, as described above for the gas-phase.

We plan to perform the QM calculations on the full reaction mechanism for the Pt(111), Pt(100), Pt(110) surfaces and determine the adsorption energy of O_2 and various intermediates (OH, HO_2) at different terrace sites (hcp, fcc, bridge, on top) and both types of step edges. Figure 10 shows O_2 at two such sites. We then use QM to examine the dissociation of the dioxygen at different sites and the migration barriers between various minima. This provides the fundamental elementary steps in the process of activating O_2 and producing H_2O. Among the terrace sites we find that dioxygen binds strongest at bridge sites. In contrast, oxygen atom prefers the threefold hollow. Clearly one must use a model catalyst surface containing all possible sites to describe properly the rates and barriers for the real catalysts. We find that such a model requires $\sim$300 atoms, too large for QM but quite straightforward for ReaxFF. With ReaxFF we can carry out MD studies to determine the effect of surface defects, step edges, kinks, impurities, alloying elements, etc. on the barriers and rates.

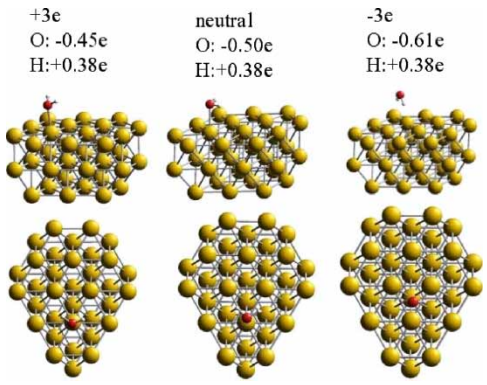

Figure 9. Structural changes due to electric field effects.

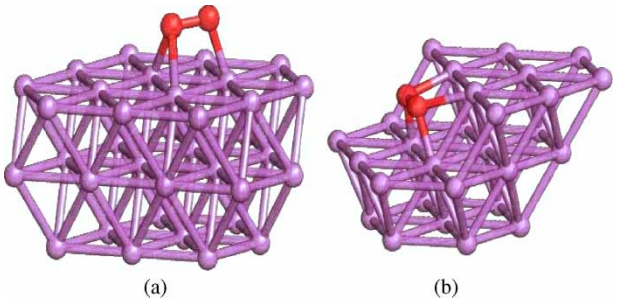

Figure 10. Adsorption of dioxygen on the fcc site (a) and on the [100] step (b).

An important factor to include is electric field enhancement [25] at step edges that may amplify the rate of the oxygen reduction reaction (ORR), the primary factor limiting the PEM-FC performance. Using ReaxFF we can impose effect field differences in different regions by fixing the net charge on the middle of the cathode catalyst particle to be negative and the middle of the anode catalyst particle to be positive. Then the charge equilibration will automatically lead to a potential gradient between them, providing appropriate field enhancement factors in the observed rates.

After predicting the rates for the gas phase reactions we can examine the rates for the catalyst covered with water and for the case, in which protons come directly from the membrane. ReaxFF calculations for the large-scale systems (10,000–1,000,000 atoms) provide the performance parameters as a function of catalyst and membrane compositions, needed for estimation of the mesoscale parameters to characterize fuel cell performance at realistic conditions.

3.3 Hydrated polymer electrolyte/cathode interface, simulations of the half-cell

We believe that the greatest challenge to understanding and optimizing PEM-FC performance is to comprehend the processes taking place at the interface between the hydrated polymer electrolyte (Nafion) and the cathode (carbon-supported Pt nanoparticles). Since the ORR occurs with protons transported from the anode through the membrane to the cathode, it is essential to understand how the protons are transferred across the membrane–cathode interface, particularly, how this is affected by the distribution of water at this interface. Although we have established that a connected (percolating) water structure exists throughout the Nafion membrane, no atomistic structural model has been proposed to explain the distribution of water and O_2 at the Pt-Nafion interface.

As the first step, we propose to predict the structures at this interface using the ReaxFF. In addition to the structural features of the interface, we will determine the dynamics of protons, O_2 molecules, and water entering the interface and reacting. We anticipate that the interface will be heterogeneous with the O_2 molecule preferring non-polar hydrophobic regions, while the proton (H_3O^+) and H_2O prefer the hydrophilic regions. Thus the

important chemistry may occur at the boundaries between these regions and the catalyst. Indeed determining the distribution and dynamics of these important species in these regions will allow us to examine how performance might be enhanced by modifying the interface between the cathode and membrane. This will likely be most important to developing new PEM-FC systems with improved performance.

To provide a basis for answering such fundamental primary questions, we have already carried out preliminary studies on a model of such an interface, including multiple phases (a hydrophobic Nafion backbone, water, O_2, and carbon support) in contact with each other as shown in figure 11(a). The Pt cathode nanoparticle is modeled using an 87-Pt atom cluster, leading to a diameter of ~ 20 Å, while the carbon support is represented using graphitic layers. We constructed this interface by integrating it with the hydrated Nafion membrane predicted previously [4]. Then this system was equilibrated using canonical ensemble MD simulations (figure 11(b)). To describe the

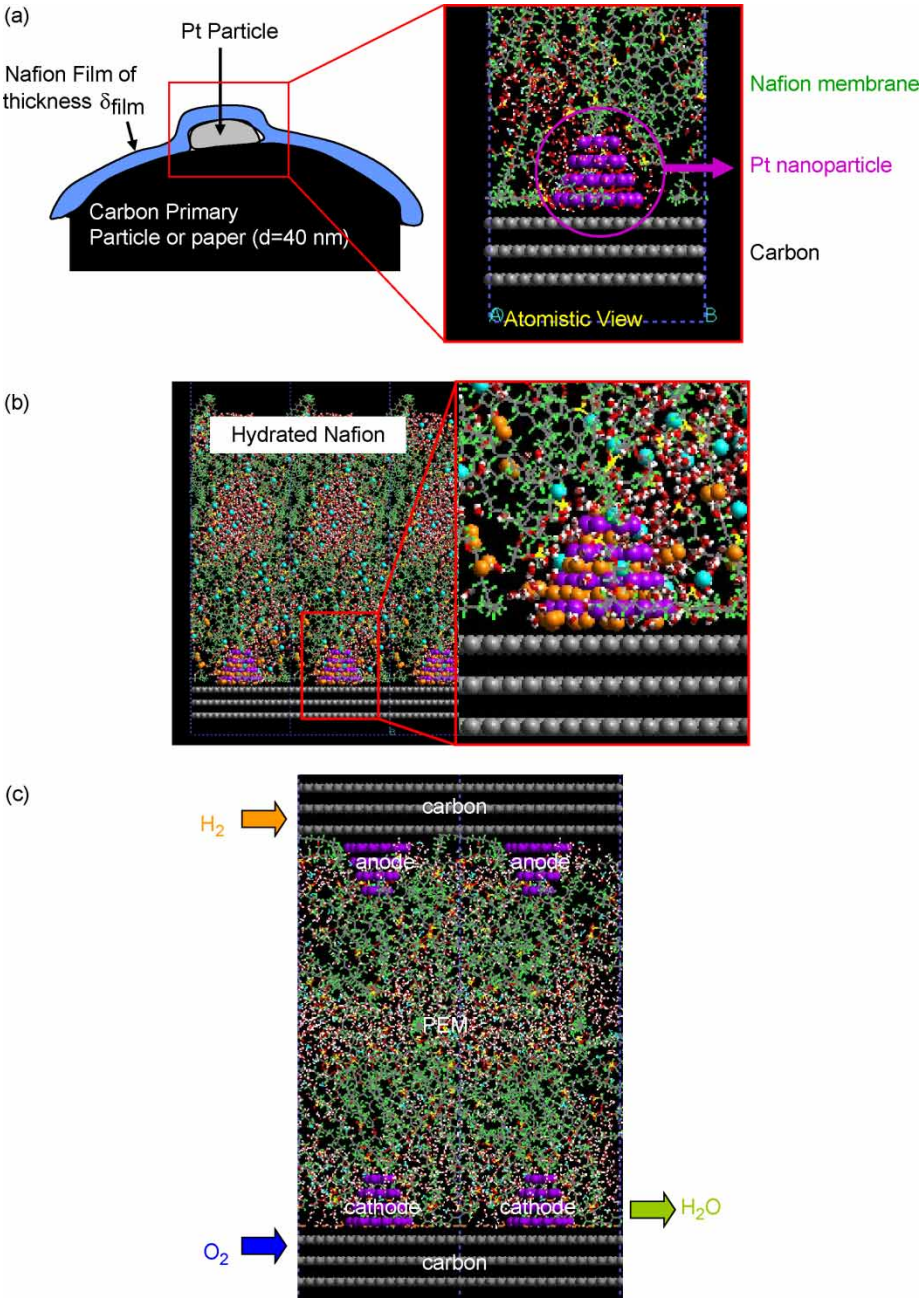

Figure 11. (a) Atomic level representation of the hydrated Nafion/cathode interface. (b) Atomistic model of the cathode interface. The orange balls are O atoms in O_2 molecules and the light blue balls are O atoms and H_3O^+ entities. (c) Atomistic model used to simulate performance of the overall PEM FC, including cathode, anode, and interfaces. The orange balls are O atoms in O_2 molecules and the light blue balls are O atoms in H_3O^+ entities. Every τ time steps an H_2 is added between the carbon layers at the top, every 2τ time steps an O_2 is added between the carbon layers at the bottom, and every τ time steps an H_2O is removed above the carbon but away from the catalysts at the bottom. The effective current is one electron every $\tau/2$ steps. The use of the ReaxFF allows the reactions at the catalysts and the migration of the protons to be described with MD studies to predict the overall fuel cell performance.

interaction of the Pt nanoparticle with other components (Nafion, water, proton and oxygen) in this MD simulation, we optimized the FF to fit the binding energy from DFT calculations at the B3LYP/6-31G** level. The FF for this Pt-cluster was optimized to reproduce such data as density, structure, and heat capacity. For Nafion and water, we used the fluorinated carbon FF [26] and the F3C water FF [27] employed successfully in previous studies of the Nafion membrane. This was also used to study a new dendrimer based alternative PEM material [28].

The MD simulation showed that the hydrated Nafion has a well-developed phase-segregated morphology with percolated water distributions reaching close to the Pt nanoparticle at the cathode. We expect that such a structure is essential for proton transport to the cathode. These simulations found that the Pt nanoparticle is entirely wetted by water, so that the proton (hydronium) particle can access the entire Pt nanoparticle surface. On the other hand, the O_2 molecules diffuse reasonably fast through the hydrophobic Nafion backbone, consistent with our expectation that the solubility of O_2 is higher in the hydrophobic Nafion backbone phase than in the water phase.

Under constant current operating conditions water molecules are generated while protons and O_2 molecules are consumed, all in the presence of electric field. This is a highly non-equilibrium system, requiring use of ReaxFF to describe the interface in such a reacting non-equilibrium state. We are currently carrying out exploratory calculations on this process. Since O_2 molecules and protons are used up while H_2O molecules are produced, we simulate the steady state process by:

(a) adding O_2 at a regular rate say every $4T$ steps between the top two layers of graphite but excluding the footprint of the catalyst and turning off the interactions of the O_2 with the top graphite layer;
(b) adding a proton to a water at the top of the diagram at a regular rate say every T steps;
(c) removing a water near the graphite but away from the catalyst at a regular rate say every $2T$ steps.

The overall current is imposed by the value of T controlling the rates of these processes. This process can be carried out for various temperatures, where we expect that the effective activation barrier will increase for higher currents.

We use a similar strategy to describe the processes at the anode–electrolyte interface and to study the properties of this half-cell as a function of current and temperatures.

Combining both processes we can describe the performance of the overall fuel cell. For the overall FC simulation (figure 11(c)) the system should be driven by controlling the rates of introducing fuel (H_2 or CH_3OH) at the anode and O_2 at the cathode and removing H_2O at the cathode. These rates determine the effective current. After steady state is achieved, we calculate the net potential difference between the two electrodes at this fixed current. Varying the rates (current) changes the overall potential leading to the fundamental performance figure of merit. This will allow us to determine how the figure of merit changes as the composition, configuration, and other conditions are modified.

4. Alternative proton conducting membranes

The conductivity of the polymeric membranes is water-assisted. To keep the water content high, the polymer electrolyte must be humidified. This limits the operating temperature of PEM-FCs to 90°C and adds further complications to the design of the fuel cell stack and system. To obtain useful rates at this low temperature requires the very best and most expensive platinum catalysts, particularly for the cathode. The choice of Pt for the anode creates additional problems since CO can poison a Pt catalyst operating at 80°C, even at concentrations of only about 50 parts per million. The poisoning could be eliminated by increasing the operating temperature to 130°C. However, the hydrated Nafion loses too much water when it operates at temperatures above 90°C.

Another serious problem for current polymer electrolytes is that they are too permeable to fuel molecules, decreasing the efficiency.

Several suggestions have been made for alternative proton conducting membranes to reduce the above problems, including:

(a) polymeric materials with heterocyclic pendant groups, such as imidazole, pyrazole, or benzimidazole;
(b) new dendrimer-PTFE copolymers combining hydrophilic dendrimers with hydrophobic linear polymers;
(c) novel Brønsted acid based ionic liquids, made by combining organic amines above their melting temperatures with bis(trifluoromethanesulfonyl) imide; and
(d) simple protic ionic liquid mixtures such as a 4:6 mixture of methyl and dimethyl ammonium nitrate that become superionic at temperature as low as 25°C.

We have already examined some of these systems as described below.

4.1 Imidazole-based water-free proton conducting membranes

As mentioned above, the very high protonic conductivity of the hydrated perfluorosulfonic polymers is due to percolating water channels surrounded by sulfonic groups to protonate the water. The proton conductivity for such systems is quite high, $\sim 10^{-1}$ S/cm for Nafion at 85°C. However, substituting water with such heterocycles, as imidazole, pyrazole, and benzimidazole has led to some cases with comparable conductivity [29].

Imidazole has a high boiling point and good proton transfer capability, suggesting it as a candidate to replace

water as a proton transfer molecule in Nafion membranes [30]. Indeed imidazole provides a very good conductivity, $\sim 10^{-1}$ S/cm at 160–180°C. Unfortunately it was found that imidazole chemisorbs on the Pt electrode, poisoning the catalyst.

Recently, we showed that fluorinated imidazole in Nafion [20] are an excellent candidate for a high temperature PEM, combining both high boiling point and conductivity required for the electrolyte while not chemisorbing on the electrode. We used QM to show that fluorinating imidazole dramatically decreases the binding energy of imidazole to Pt (from 21.1 to 1.3 kcal/mol for trifluoroimidazole), to a value much lower than the binding energy for water on Pt (12.5 kcal/mol).

Moreover, we calculated the proton diffusion in the trifluoroimidazole/Nafion membrane to be only 40% lower than that of imidazole/Nafion at the same temperature and concentration. This comparison of the proton diffusivities was done by a combined QM/MD approach we developed for such calculations. In this approach, we compute the vehicular diffusion component from the classical MD simulations using non-reactive FF with explicit H_3O^+ entities. Then we calculate the hopping diffusion term using the configurations from the MD and evaluating the proton hop rates using transition state theory (TST) with quantum tunneling correction based on energy curves for proton transfer completely computed from *ab initio* QM. Thus trifluoroimidazole is a promising candidate for water replacement.

The method used above to estimate proton diffusion rates in the bulk electrolyte is simple and efficient way, but it is not suitable for describing details of proton transfer at the electrolyte–catalyst interface. We intend to use ReaxFF MD methodology, allowing explicit proton hopping to obtain the rates.

4.2 Dendrion polymeric materials combining hydrophilic dendrimer and hydrophobic PTFE

Current state-of-the-art PEM-FC technologies are based on the hydrated perfluorosulfonic polymers such as Nafion, which has a high proton conductivity as well as excellent chemical and thermal stability. These favorable properties result from the nanophase-segregated structure consisting of two phases: one is the hydrophobic phase of perfluorinated polymer backbone and the other is the hydrophilic water phase associated with sulfonic groups belonging to polymer. In previous studies [4], we found that the nanophase-segregated structure can be controlled by specifying the molecular architecture (monomeric sequence and cross linking), which in turn determines the transport characteristics of PEMs.

Recently we proposed the Dendrion copolymer in which a water-soluble polyaryl ethereal dendrimer (Fréchet type dendrimer [31]) is covalently bound with a hydrophobic linear PTFE. From such molecular constituents we expected that this copolymer would form a nanophase-segregated structure with a specific amount of water available for proton transport. We also expected that the polar groups were localized at the surface of the dendrimer through covalent connectivity, leading to formation of a well-defined spatial distribution of polar group in the membrane. Since the transport properties of the membrane are coupled with its nanostructure, we may systematically control the transport properties by managing water distribution through nanophase segregation in the membrane. Many factors affect the nanophase segregation (dendrimer size, type of acid groups, equivalent weight of copolymer), but our initial studies focused on the water content and distribution as a function of temperature, since this is critical to good performance.

We carried out MD simulations to determine the structure and properties of the Dendrion hydrated copolymer membrane consisting of the second-generation Fréchet type dendrimer combined with linear PTFE copolymer (1100 of equivalent weight) to assess the effect of water content on the nanophase-segregated structure and transport properties.

We prepared two model systems each of the same dendrimer-PTFE copolymer chains but with different water contents (5 and 10 wt%). Then we carried out MD simulations under the conditions previously used for Nafion: 1 atm and 353.15 K. We found that nanophase segregation, which appeared during the pressure–temperature annealing procedure, used to determine the equilibrium structure of such amorphous polymers (figure 12). We also examined the structure and the transport properties from a 5 ns equilibrium NPT MD simulation.

Analyzing the water structure in the Dendrion, we found that the water phase formed bulk-water-like connected channels more efficiently, than in the Nafion membrane. We expect that this bulk-water-like structure will facilitate proton hopping as easily as for the bulk water.

We calculated a water diffusion coefficient of 0.37×10^{-5} cm^2/s (10 wt% water content) and 0.21×10^{-5} cm^2/s (5 wt% water content), which is 4–7 times smaller than in Nafion membrane ($\sim 1.5 \times 10^{-5}$ cm^2/s). This suggests that the Dendrion may have a smaller electro-osmotic drag coefficient than Nafion.

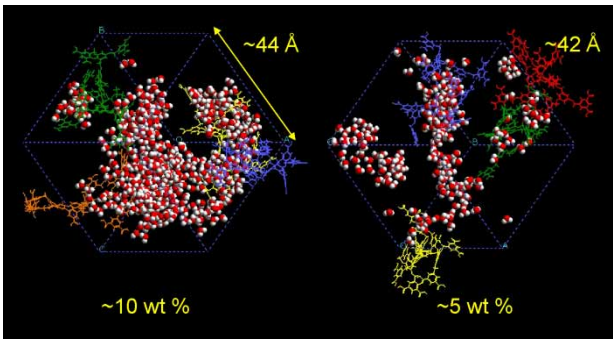

Figure 12. Predicted nanophase segregated structure of the dendrion hydrated Fréchet dendrimer-PTFE copolymer membrane.

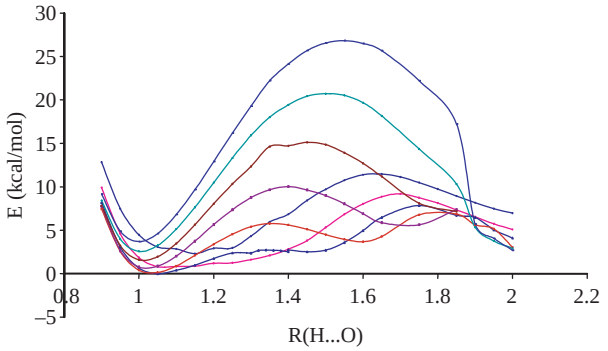

Figure 13. Proton transfer barriers as a function of R(H···O) distance (in Å) in the methylethylammonium nitrate ionic liquid.

These structural and dynamical features of the dendrion membrane make it a promising candidate for FC applications [28].

4.3 Ionic liquids

Just recently it was recognized that ionic liquids can serve as proton conducting non-aqueous electrolytes in FCs. Novel Brønsted acid based ionic liquids made by combining imidazole with bis(trifluoromethanesulfonyl) imide (HTFSI) are promising candidate materials for fuel cell applications [32]. They are electroactive for H_2 oxidation and O_2 reduction at the Pt electrode under non-humidifying conditions at moderate temperatures (~130°C). Other very promising materials are simple protic ionic liquid mixtures (such as a 4:6 mixture of methyl and dimethyl ammonium nitrate) that become superionic at 25°C. At 25°C the conductivity is similar to Nafion at 80°C (0.15 vs. 0.1 S/cm), but at 100°C the conductivity of the ionic liquid system is of 0.47 S/cm, 4 times larger than for Nafion.

In order to provide a basis for understanding the superprotonic conductivity of ionic liquids, we determined the QM barrier for proton transfer in the methyl–ethyl ammonium nitrate system (figure 13). For hydrogen bonds shorter than 2.5 Å there is essentially no barrier for proton transfer, which is likely an important factor in explaining the superionic nature of this ionic liquid.

For these systems to be used in a commercial FC, we want to anchor the anion of the ionic liquid to an immobile phase, preferably a high temperature stable polymer. A variety of ionic liquids (such as in figure 14) will be screened and then the most promising candidates will be selected for further study. We consider that such anhydrous protonic materials offer excellent opportunities for improved FC materials. It is important to determine the fundamental physics and chemistry of the proton conducting phenomena in this vast under explored class of materials. This will provide critical data needed to design protonic materials that can operate at moderate temperatures (100–200°C), to attain significant gains in efficiency (conductivity), low toxicity and high thermal stability, and compatibility with the electrode catalyst. We will implement multi-scale tools for quantum hopping molecular dynamics (QHMD) methods to simulate both quantum and classical events in proton transfer reactions, including new first principles-based FFs capable of proton transfer events.

5. Electrode alloy catalyst materials for PEM-FCs

5.1 Atomic scale design of advanced alloy anode catalysts

Although platinum is currently the best anode electrocatalyst for PEM-FCs, it suffers from CO poisoning. Therefore, it is highly desirable to develop new anode catalysts with higher CO tolerance. Ruthenium (Ru) alloyed Pt with the atomic ratio of 1:1 is known to be effective in CO removal and to significantly promote FC performance. In addition, the $Pt_{50}Ru_{50}$ alloy on a PEM is currently the best anode catalyst for direct methanol fuel cell (DMFC) [33–35].

The mechanism widely accepted for the CO oxidation [11,36] on PtRu is:

$$\mathrm{Ru + H_2O \rightarrow Ru{-}OH + H_{add}};$$

$$\mathrm{Pt{-}CO + Ru{-}OH \rightarrow Pt + Ru + CO_2 + H_{add}},$$

where the rate-determining step is the formation of Ru–OH species [37]. The relatively easy formation of hydroxides (RuOH) or hydrous oxides (RuO_xH_y) of oxyphilic Ru probably plays a key role in preventing the CO poisoning of Pt. Ru is well known [11] for its water-dissociating capability and rich oxygen chemistry. Thus chemisorbed

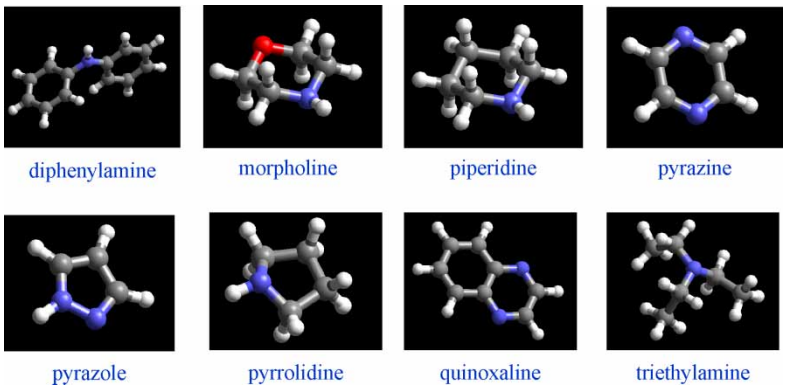

Figure 14. Examples of proton acceptor for a Brønsted acid bis(trifluoromethanesulfonyl) for non-aqueous proton transfer membrane media.

oxygen, surface oxide, subsurface oxygen, and buried oxides may coexist in the near-surface region [38,39]. It has been reported that Pt remains metallic under operating conditions, while Ru forms oxides, hydroxides, or amorphous hydrous oxides during the electrocycle [40,41].

However, there remain controversies on the exact nature of the promotion mechanism, both on the nature of active Ru species [metallic ruthenium (Ru), ruthenium oxides (RuO_2 and RuO_3), hydroxides (RuOH) or hydrous oxides (RuO_xH_y)], and also on how the OH species bound to Ru more strongly than to Pt can spillover to a neighboring Pt sites and combine with CO there. Possibly it picks up a hydrogen from a water molecule on a neighboring Pt atom, effectively a transfer of OH from Ru to Pt [42]. Therefore, it is important for designing the most active Pt–Ru electrocatalysts to have

- the optimum Pt–Ru surface concentration,
- the optimum Pt–Ru distribution and structure,
- the optimum water content around the active sites.

The surface composition and structure of the alloy catalyst affect the activity and selectivity. This depends drastically on such experimental conditions as the synthesis temperature and subsequent processing conditions that make complicate to extract an atomistic interpretation of the experimental activity. We use theory and computation to interpret experiments by determining the atomic level reaction mechanisms and energetics for various plausible surface structures and compositions, including the boundary between the Pt–Ru solid solution phase and the hydrous ruthenium oxide phase.

We investigate the oxygen and water chemistry of hydrous Ru and RuO_x surfaces (step 1: $Ru/RuO_x/RuO_xH_y$), and then mix them with Pt (step 2: $Pt–Ru/RuO_x/RuO_xH_y$) in order to pin down the active sites for oxygen/water activation and for CO oxidation to CO_2. This allows us to deduce which arrangement of Pt, Ru, and their oxides/hydroxides/hydrous oxides, and possibly the other alloying elements, can form appropriate active sites to reduce the energy barrier of the critical steps. We use the first-principles calculations to elucidate:

(a) surface compositions and structures of metal/metal oxide alloys, including surface defects, for various environments (oxygen, water, etc.; surface/subsurface oxide, hydroxide, or hydrous oxide formation);
(b) each step from activation of the fuel (H_2) and the poison (CO) and how this depends on surface defects and alloying;
(c) how each of these steps is affected by solvation and electric fields.

All previous theoretical studies have been limited to ideal metal surfaces or ideal surfaces of Pt–Ru solid solution phases [43–48]. We intend to simulate the evolution of "realistic" Pt–Ru alloy surfaces at operating conditions, including surface hydration and oxidation.

It is important to study the surface segregation of Pt, how the segregation changes under a variety of oxidation conditions, the effect of lattice strain (compressive or expansive) as a result of the alloying process, and the electronic coupling of the Pt-skin layer with the alloy substrate. This should provide insight on the fundamental origin of the reactivity difference between the alloys and pure Pt.

Since CO poisoning represents one of the major problems for the catalysis on Pt-DMFC anodes, we plan to study the effect of alloying (PtRu, PtIr, PtOs, PtMo) on the MeOH chemistry. Our goal is to develop insight into the effect of the electronic structure on specific bond breaking events, which would be useful for guiding the catalyst discovery to more promising areas of the complicated alloy phase diagrams. Similarly, our DFT calculations can provide detailed information on the adsorbate/alloy-induced change in the electronic structure of the catalytic surface, the structure of surface reactive intermediates, and diffusion barriers.

Along with our studies of the MeOH chemistry on Pt and its alloys, we probe the effect of water on that chemistry as a function of the electronic structure of the substrate. Water is present at the anode of DMFCs under realistic operating conditions and this part of our investigations will address key mechanistic issues of the anode reactivity. H_2O is expected to alter the interaction of MeOH and its derivate reaction intermediates with the catalytic surface in a substantial way. Besides changing the potential energy characterizing the MeOH/Pt interaction, new reaction paths would become available to these intermediates. One of the most interesting parts of this research is to determine the interaction of CO and H_2O at the anode. As MeOH represents the first member of hydrocarbons, which can be reformed through the aqueous phase hydrocarbons reforming (ACR) process to hydrogen, our studies of the MeOH reactivity on the anode catalyst would directly benefit our studies of the ACR process. Pt represents one of the most promising catalysts for the anode of DMFCs and for the ACR process. Therefore, reactivity of oxygenates on Pt and Pt-based alloys would have an impact on both subjects.

We also plan to study the MeOH decomposition on stepped Pt surfaces, which is critical for addressing particle size effects relevant to the anode catalysis of DMFCs. In particular, the mechanism of MeOH decomposition will be studied on the Pt(211) surface, presenting a more reactive step edge, which could serve as a model for defect sites on the catalyst.

5.2 Atomic scale design of advanced alloy cathode catalysts

The PEM-FC performance is limited most by the ORR kinetics and second by transport losses due to proton conduction in the cathode catalyst layer and oxygen transport to the cathode catalyst. Therefore, optimization of the electrocatalytic processes at the cathode could significantly improve fuel cell performance. Some results showing activity gains have been reported in the literature

on binary alloy catalysts, such as PtNi, PtCo, and PtCr [49] as well as ternary alloy catalysts [50]. However, these have not been implemented widely in FC stacks yet.

To make progress in developing improved catalysts, it is important to understand the fundamental processes for these catalysts. We studied Pt_3Ni and Pt_3Co, since both provide improved performance relative to pure Pt. We find that the bulk alloy has only Pt neighbors to each Ni or Co, which for the surface would lead to 1/4 of the surface atoms being Ni or Co. However, QM calculations for the two-dimensional periodic slabs shows that the most stable surface has no Ni or Co on the surface. Apparently the preference for Ni or Co to have 12-Pt neighbors is strong enough to drive what would have been surface Ni or Co to the second layer. The result is 100% Pt in the top layer, 50% in the second layer and then 75% in the third and subsequent layers. This has also been observed experimentally. Although there are no Ni or Co in the top layer, the chemical activity of the surface Pt is dramatically affected by where the second layer Ni or Co are located. This is shown in figure 15, where one can see that the energy surface for movement of chemisorbed O and H is quite corrugated [5], with H surface coverage much higher barriers than for pure Pt. Oxygen has a hopping barrier of $\sim$2 eV, compared to $\sim$0.6 eV for the pure Pt(111) surface. Thus on the alloy surface oxygen is strongly localized. Similarly, hydrogen is known to be very mobile on the Pt surface, with diffusion barriers of only $\sim$0.1 eV. However, for the Pt/Ni alloy we found that the hydrogen atoms were much less mobile leading to "channels" between and on circles around the Ni atoms (figure 15). The nearly fixed oxygen location and the constrained hydrogen mobility may increase the probability that both atoms come close enough to react with each other. This example shows how alloying significantly changes the system character and has a dramatic effect on the barriers for the various reaction steps discussed in figure 7. In particular, we expect that the barrier for O_2 dissociation will decrease because of charge transfer from second layer Ni or Co to the surface Pt, making formation of chemisorbed O_2 more favorable.

We have also studied finite clusters for the Pt_3Ni alloy and found these results to be quite different than in the infinite slab. Ni atoms are found at the surface with the same distributions as if they were cut from the infinite crystal. Therefore, clusters are not large enough for the top layer to be pure Pt. For clusters less than 4 nm on a side, we expect the surface chemistry to be quite different than for the bulk.

The QM calculations described above are essential to determine accurate barriers and pre-exponential factors. However, for simulating complex processes on realistic surfaces as a function of temperature and the dependence on the nature of the catalyst–electrolyte interface, we must carry out MD simulations for at least ns on systems with many thousands of atoms. We extend ReaxFF to describe the various cathode catalytic processes on Pt alloy systems.

6. Summary

A great deal of progress has been made over the last decade in developing fuel cells with increased efficiency and decreased cost, but the current generation remains well

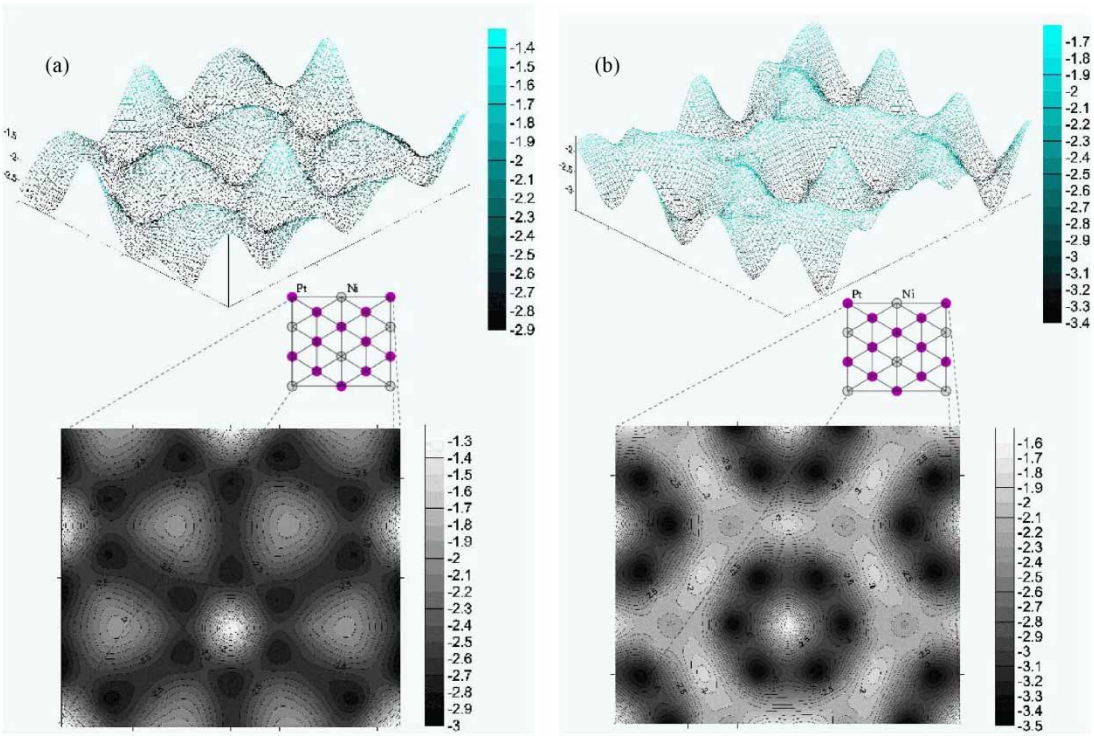

Figure 15. (a) Energy surface (eV) for migration of chemisorbed H atom on the $Pt_3Ni(111)$ alloy surface; (b) same for O atom.

short of the needs of society. We propose to address such problems using recently developed rational approaches based on first principles predictions. This uses the new first-principles based reactive ReaxFF force field to describe chemical processes (ion, proton and water transfer, oxygen reduction, reactions of intermediates, phase transformations, etc.) at a scale suitable to address the issues of anode catalysis, cathode catalysis, proton-conducting polymer electrolytes, and electrode/electrolyte interfaces. We focus on overcoming some key bottlenecks in this process and are now at the point where building these techniques into an integrated computational facility and applying them to the fundamental processes at the anode and cathode catalysts, in the proton-conducting electrolyte connecting them, in the interfaces between these elements, and in the fuel processing would enable the conception, synthesis, fabrication, development, and understanding of advanced materials and structures for PEM-FCs.

Acknowledgements

This work was partially sponsored by General Motors. The computation facilities of the MSC have been supported by grants from DURIP-ARO, DURIP-ONR, NSF (MRI), and IBM-SUR. In addition, the MSC is supported by grants from DOE (DE-FG01-04ER04-20 and DE-FC26-02NT41631), ARO-MURI, ONR-MURI, NIH, ONR (NO. 014-02-1-0665), Chevron-Texaco, and Beckman Institute.

References

[1] K. Chenoweth, S. Cheung, A.C.T. van Duin, W.A. Goddard, E.M. Kober. Simulations on the thermal decomposition of a poly(dimethylsiloxane) polymer using the ReaxrFF reactive force field. *J. Am. Chem. Soc.*, **127**, 7192 (2005).

[2] K.D. Nielson, A.C.T. van Duin, J. Oxgaard, W. Deng, W.A. Goddard III. Development of the ReaxFF reactive force field for describing transition metal catalyzed reactions, with application to the initial stages of the catalytic formation of carbon nanotubes. *J. Phys. Chem. A*, **109**, 493 (2005).

[3] T. Jacob, W.A. Goddard III. Adsorption of atomic H and O on the (111) surface of Pt3Ni alloys. *J. Phys. Chem. B*, **108**, 8311 (2004).

[4] S.S. Jang, V. Molinero, T. Cagin, W.A. Goddard III. Nanophase-segregation and transport in Nafion 117 from molecular dynamics simulations: effect of monomeric sequence. *J. Phys. Chem. B*, **108**, 3149 (2004).

[5] T. Jacob, B.V. Merinov, W.A. Goddard III. Chemisorption of atomic oxygen on Pt(111) and Pt/Ni(111) surfaces. *Chem. Phys. Lett.*, **385**, 374 (2004).

[6] X. Xu, W.A. Goddard III. The X3LYP extended density functional for accurate descriptions of nonbond interactions, spin states, and thermochemical properties. *Proc. Natl. Acad. Sci. USA*, **101**, 2673 (2004).

[7] J. Timo, R.P. Muller, W.A. Goddard III. Chemisorption of atomic oxygen on Pt(111) from DFT studies of Pt-clusters. *J. Phys. Chem. B*, **107**, 9465 (2003).

[8] P.A. (unpublished) for a description of the method see: P.J. Feibelman Schultz. Force and total energy calculations for a spatially compact adsorbate on an extended, metallic crystal surface. *Phys. Rev. B***35**, pp. 2626–2646 (1987)

[9] V.R. Saunders, R. Dovesi, C. Roetti, R. Orlando, C.M. Zicovich-Wilson, N.M. Harrison, K. Doll, B. Civalleri, I. Bush, Ph. D'Arco, M. Llunell. *CRYSTAL User's Manual*, University of Torino, Torino (2003).

[10] A.C.T. van Duin, S. Dasgupta, F. Lorant, W.A. Goddard III. ReaxFF: a reactive force field for hydrocarbons. *J. Phys. Chem. A*, **105**, 9396 (2001).

[11] A. Strachan, A.C.T. van Duin, D. Chakraborty, S. Dasgupta, W.A. Goddard III. Shock waves in high-energy materials: the initial chemical events in nitramine RDX. *Phys. Rev. Lett.*, **91** (2003) (article no. 098301).

[12] A.C.T. van Duin, Y. Zeiri, F. Dubnilova, R. Kosloff, W.A. Goddard. Atomistic-scale simulations of the initial chemical events in the thermal initiation of triacetonetriperoxide. *J. Am. Chem. Soc.*, **127**, 11053 (2005).

[13] Q. Zhang, T. Cagin, A.C.T. van Duin, W.A. Goddard, Y. Qi, L.G. Hector. Adhesion and nonwetting–wetting transition in the Al/alpha–Al2O3 interface. *Phys. Rev. B*, **69** (2004) (article no. 045423).

[14] A.C.T. van Duin, A. Strachan, S. Stewman, Q. Zhang, W.A. Goddard III. ReaxFF sio reactive force field for silicon and silicon oxide systems. *J. Phys. Chem. A*, **107**, 3803 (2003).

[15] S. Cheung, W. Deng, A.C.T. van Duin, W.A. Goddard III. ReaxFF(MgH) reactive force field for magnesium hydride systems. *J. Phys. Chem. A*, **109**, 851 (2005).

[16] S.S. Han, A.C.T. van Duin, W.A. Goddard, H.M. Lee. Optimization and application of lithium parameters for the reactive force field, ReaxFF. *J. Phys. Chem. A*, **109**, 4575 (2005).

[17] N. Chen, M.T. Lusk, A.C.T. van Duin, W.A. Goddard III. Mechanical properties of connected carbon nanorings via molecular dynamics simulation. *Phys. Rev.B*, **72** (2005) (article no. 085416).

[18] W.A. Goddard III, Q. Zhang, M. Uludogan, A. Strachan, T. Cagin. The ReaxFF polarizable reactive force fields for molecular dynamics simulation of ferroelectrics. In *Fundamental Physics of Ferroelectrics*, R.E. Cohen (Ed.), (2002).

[19] A. Nakano, R.K. Kalia, K. Nomura, A. Sharma, P. Vashista, F. Shimojo, A.C.T. van Duin, W.A. Goddard III, R. Biswas, D. Srivastava. Million-to-billion atom simulation of chemical reactions: embedded divide-and-conquer and hierarchical cellular decomposition frameworks for scalable scientific computing. *Submitted to IEEE/ACM Supercomputing Proceedings*, (2005).

[20] W. Deng, V. Molinero, W.A. Goddard III. Fluorinated imidazoles as proton carriers for water-free fuel cell membranes. *J. Am. Chem. Soc.*, **126**, 15644 (2004).

[21] T.D. Gierke, G.E. Munn, F.C. Wilson. The morphology in Nafion perfluorinated membrane products, as determined by wide-angle and small-angle X-ray studies. *J. Polym. Sci.: Polym. Phys.*, **19**, 1687 (1981).

[22] D.H. McAdon, W.A. Goddard III. New concepts of metallic bonding based on valence bond ideas. *Phys. Rev. Lett.*, **55**, 2563 (1985).

[23] J. Kua, W.A. Goddard III. Chemisorption of organics on platinum. *J. Phys. Chem.*, **102**, 9481 (1998).

[24] T. Jacob, W.A. Goddard III. Chemisorption of (CHx and C2Hy) hydrocarbons on Pt(111) clusters and surfaces from DFT studies. *J. Phys. Chem. B*, **109**, 297 (2005).

[25] R. Monreal, S.P. Apell. Electromagnetic-field-enhanced desorption of atoms. *Phys. Rev. B*, **41**, 7852 (1990).

[26] S.S. Jang, M. Blanco, W.A. Goddard III, G. Caldwell, R.B. Ross. The source of helicity in perfluorinated *N*-alkanes. *Macromolecules*, **36**, 5331 (2003).

[27] M. Levitt, M. Hirshberg, R. Sharon, K.E. Laidig, V. Daggett. Calibration and testing of a water model for simulation of the molecular dynamics of proteins and nucleic acids in solution. *J. Phys. Chem. B*, **101**, 5051 (1997).

[28] S.S. Jang, S.-T. Lin, T. Cagin, V. Molinero, W.A. Goddard III. Nanophase segregation and water dynamics in the dendrion diblock copolymer formed from the Frechet polyaryl ethereal dendrimer and linear PTFE. *J. Phys. Chem. B*, **109**, 10154 (2005).

[29] K.-D. Kreuer, A. Fuchs, M. Ise, M. Spaeth, J. Maier. Imidazole and pyrazole-based proton conducting polymers and liquids. *Electrochim. Acta*, **43**, 1281 (1998).

[30] C. Yang, P. Costamagna, S. Srinivasan, J. Benziger, A.B. Bocarsly. Approaches and technical challenges to high temperature operation of proton exchange membrane fuel cells. *J. Power Sources*, **103**, 1 (2001).

[31] C.J. Hawker, K.L. Wooley, J.M.J. Frechet. Unimolecular micelles and globular amphiphiles - dndritic macromolecules as novel recyclable solubilization agents. *J. Chem. Soc., Perkin Trans.*, **1**, 1287 (1993).

[32] A. Noda, M.A.B.H. Susan, K. Kudo, S. Mitsushima, K. Hayamizu, M. Watanabe. Bronsted acid–base ionic liquids as proton-conducting nonaqueous electrolytes. *J. Phys. Chem.*, **107**, 4024 (2003).

[33] H. Kim, I.R. de Moraes, G. Tremiliosi-Filho, R. Haasch, A. Wieckowski. Chemical state of ruthenium submonolayers on a Pt(111) electrode. *Surf. Sci. Lett.*, **474**, L203 (2001).
[34] L. Giorgi, A. Pozio, C. Bracchini, R. Giorgi, S. Turtu. H-2 and H-2/CO oxidation mechanism on Pt/C, Ru/C and Pt−Ru/C electrocatalysts. *J. Appl. Electrochem.*, **31**, 325 (2001).
[35] C.Z. He, H.R. Kuntz, J.M. Fenton. Electro-oxidation of hydrogen with carbon monoxide on Pt/Ru-based ternary catalysts. *J. Electrochem. Soc.*, **150**, A1017 (2003).
[36] M. Watanabe, S.J. Motoo. Electrocatalysis by ad-atoms.2. Enhancement of oxidation of methanol on platinum by ruthenium ad-atoms. *J. Electroanal. Chem.*, **60**, 267 (1975).
[37] A. Kabbabi, R. Faure, R. Durant, B. Bedan, F. Hahn, J.-M. Leger, C. Lamy. *In situ* FTIRS study of the electrocatalytic oxidation of carbon monoxide and methanol at platinum−ruthenium bulk alloy electrodes. *J. Electroanal. Chem.*, **444**, 41 (1998).
[38] P.J. Feibelman. Partial dissociation of water on Ru(0001). *Science*, **295**, 99 (2002).
[39] H. Over, A.P. Seitsonen. Oxidation of metal surfaces. *Science*, **297**, 2003 (2002).
[40] R. Liu, H. Iddir, Q. Fan, G. Hou, A. Bo, K.L. Ley, E.S. Smotkin, Y.-E. Sung, H. Kim, S. Thomas, A. Wieckowski. Potential-dependent infrared absorption spectroscopy of adsorbed CO and X-ray photoelectron spectroscopy of arc-melted single-phase Pt, PtRu, PtOs, PtRuOs, and Ru electrodes. *J. Phys. Chem. B*, **104**, 3518 (2000).
[41] C. Roth, N. Martz, H. Fuess. Characterization of different Pt−Ru catalysts by X-ray diffraction and transmission electron microscopy. *Phys. Chem. Chem. Phys.*, **3**, 315 (2001).
[42] M.T.M. Koper. Electrocatalysis on bimetallic and alloy surfaces. *Surf. Sci.*, **548**, 1 (2004).
[43] T.E. Shubina, M.T.M. Koper. Quantum-chemical calculations of CO and OH interacting with bimetallic surfaces. *Electrochim. Acta*, **47**, 3621 (2002).
[44] Y. Ishikawa, M.-S. Liao, C.R. Cabrera. Energetics of H2O dissociation and COads+OHads reaction on a series of Pt−M mixed metal clusters: a relativistic density-functional study. *Surf. Sci.*, **513**, 98 (2002).
[45] S. Desai, M. Neurock. A first principles analysis of CO oxidation over Pt and Pt66.7%Ru33.3% (111) surfaces. *Electrochim. Acta*, **48**, 3759 (2003).
[46] S.K. Desai, M. Neurock. First-principles study of the role of solvent in the dissociation of water over a Pt−Ru alloy. *Phys. Rev. B*, **68**, 75420 (2003).
[47] P. Liu, A. Logadottir, J.K. Norskov. Modeling the electro-oxidation of CO and H-2/CO on Pt, Ru, PtRu and Pt3Sn. *Electrochim. Acta*, **48**, 3731 (2003).
[48] M. Christov, K. Sundmacher. Simulation of methanol adsorption on Pt/Ru catalysts. *Surf. Sci.*, **547**, 1 (2003).
[49] S. Mukerjee, S. Srinivasan. Enhanced electrocatalysis of oxygen reduction on platinum alloys in proton-exchange membrane fuel cells. *J. Electroanal. Chem.*, **357**, 201 (1993).
[50] S. Gamburzev, O.A. Velev, S. Srinivasan, A.J. Appleby, F.J. Luczak, D. Wheeler. *Carbon Supported Ternary Platinum Alloys Oxygen Reduction Catalysts for PEM-FCs*, Montreal (1997).